

Lawrence Berkeley National Laboratory

LBL Publications

Title

Shape transformation and self-alignment of Fe-based nanoparticles

Permalink

<https://escholarship.org/uc/item/8q01k1cv>

Journal

Nanoscale Advances, 1(7)

ISSN

2516-0230

Authors

Hong, Jeongmin

Luo, Qiang

Jung, Daesung

et al.

Publication Date

2019-07-09

DOI

10.1039/c9na00146h

Peer reviewed

Shape transformation and self-alignment of Fe based nanoparticles

Abstract: New types of functional material structures will be emergent by the controllability of the shape and properties in 3D nanodevices. Possible applications would be nanoelectronics and medical systems. Magnetic nanoparticles (MNPs) are especially important in electronics such as magnetic storage, sensors, and spintronics. Also, those are used as magnetic resonance imaging contrasts, and tissue-specific therapeutic agents, as well as in the labeling and sorting of cells, drug delivery, separation of biochemical products, and other medical applications. Most of these applications require the magnetic nanoparticles to be chemically stable, uniform in size, and controllable in terms of their magnetic properties and shape. We report three new functions of Fe-based nanoparticles: shape transformation, oxidation prevention, and self-alignment. Fe nanoparticles could be controllable for their shape by oxidation states and properties through nanocarbon coating. Full field x-ray microscopy using synchrotron radiation revealed controllable magnetic properties of MNPs at L_3 edge depending on the oxide states. Then, inkjet printing was successfully performed to deposit the uniform layer of MNPs depending on the size by drying the layer of nanoparticles.

Recent development of nanoparticles ranges from chemistry, physics, biosciences, materials science, and many others.^[1-6] Due to the widespread applications of magnetic nanoparticles (MNPs) in biotechnology, materials science, engineering, and environmental studies,

much attention has been paid to the controllable synthesis of different types of MNPs.^[4] The applications are ferrofluids, recording media, magnetic refrigeration, magnetic resonance imaging, drug delivery, cancer therapy, and many other applications.^[7-10]

MNPs usually exhibit superparamagnetic behavior because of their infinitely small coercivity as their sizes are reduced down to sub-10-nm range. For example, one of the important applications of superparamagnetic NPs is their use as drug-delivery agents to overcome the blood brain barrier (BBB) under controllable magnetic fields.^[11] However, MNPs tend to aggregate into large clusters, and thus, lose specific properties associated with single-domain magnetic nanostructures.^[12] Therefore, a new efficient approach to achieve adequately controllable magnetic properties of MNPs needs to be investigated.

Fe shows superior magnetic properties which are important for spintronics and nanomedicine. However, it is easily oxidized to lose its properties by phase transitions. Pure Fe nanoparticles covered by nanocarbon shell structures such as carbon nanotubes (CNT) and graphene could not only protect the oxidation, but manipulate carbon's physical properties.^[13] The production of pure Fe nanoparticles is challenging, but after systematic synthesis of nanocarbon shell, the properties of Fe can be present without further oxidation.^[14,15] The use of superior properties of nanocarbon structures and interfaces could be useful for many applications through magneto-electric (ME) effects.^[16-18]

Although the use of nanoparticles in the solution is well controllable, MNPs are very challenging to align them in a dry form due to its interactions between MNPs.^[16] Drop cast and spray methods are very common use to deposit MNPs onto the substrates. Inkjet printing technology opens a way to align in multiple dimensions. Printing MNPs makes it possible to align in 2D and 3D structures if it is deposited in a controllable way.^[19] Through the optimal condition for inkjet printing, a drop of liquid's suspended particulate matter is deposited in ring-like fashion on the substrate. The effects could control the alignment of same size distribution of the nanoparticles by the fluid dynamics.

Here, we present a unique way to modulate MNPs by controlling the size, shape, and magnetic properties. To prevent oxidation, nanocarbon shell was covered on Fe structures. In the case of oxide and pure Fe states, magnetic properties of nanocarbon are not well studied by characterizing magnetometry.^[20,21] Magnetic microscopy such as MFM limits phase imaging due to its topographical effects of MNPs as described in **Supplementary Information**. Using synchrotron radiation, full field x-ray microscopy was successfully performed to present element specific magnetic imaging through x-ray magnetic circular dichroism (XMCD). Fe based particles imaging could distinguish pure Fe and Fe-O at L_3 edge. Then, the particles were printed onto the rigid and even flexible substrates using inkjet printing technology.

We started from magnetite nanoparticles obtained by the conventional method.^[21] The size of the magnetic nanoparticles varied from 5 to 200 *nm* as shown in **Figure 1**. From the results of the coagulation experiment,

it was found that the particles coagulate very easily by applying magnetic field. The coagulation of MNPs are a more stable state if the coagulation stabilizes. When the fabrication conditions such as pH and process temperature were changed, the particles transformed to other stable forms of iron oxide, such as maghemite ($\gamma\text{-Fe}_2\text{O}_3$) and hematite ($\alpha\text{-Fe}_2\text{O}_3$). Five types of shape transformation of MNPs were observed: pyramidal, square, hybrid (coexisting with circular and square structures), and oval structures as reported in other literature.^[22]

The controllable synthesis of nanocrystalline iron oxide, particularly, of pyramidal shape of MNPs was performed. **Figures 1a-f** illustrate the transformation cycle. The initial magnetite is oxidized to the transition state before pyramid formation, and then is transformed into the square structure. After further oxidation, this structure changed to hybrid states from the circular, square, and oval structures, and finally saturated in the mixed states. *It must be noted that the different oxidation levels during synthesis result in the coarsening of the precipitated nanoparticles.*

Bi-pyramidal structures are the most common structures as reported.^[23,24]

*However, single pyramid is also very important especially for magnetic sensors to focus magnetic field along the direction of the apex. Ideally, formed octahedral and tetrahedral structures, indicative of the formation of self-assembled pyramidal nanodevices, can be seen in the x-ray diffraction patterns shown in **Supplementary Information**. We found a unique combination of octahedral and tetrahedral lattice structures, resulting in perfectly shaped pyramidal pits of iron oxide MNPs.*

Vibrating sample magnetometry shows superparamagnetic behavior with regards to the levels of oxidation, as shown in **Figure 1c**. The structure is unique for an intense magnetic field generation and sensing because of octahedral driven by the demand of shape-controlled synthesis of $\alpha\text{-Fe}_2\text{O}_3$ nanostructures and shape-dependent properties. The synthesis of octadecahedral $\alpha\text{-Fe}_2\text{O}_3$ nanocrystals with a hexagonal pyramid shape by packing of truncated nanodots into several different superstructures. The findings are of fundamental importance to understand the morphology and growth of $\alpha\text{-Fe}_2\text{O}_3$ nanostructures. The better control of the shape evolution of hematite particles will provide direct correlation between exposed facets and facet-controlled properties in future study.

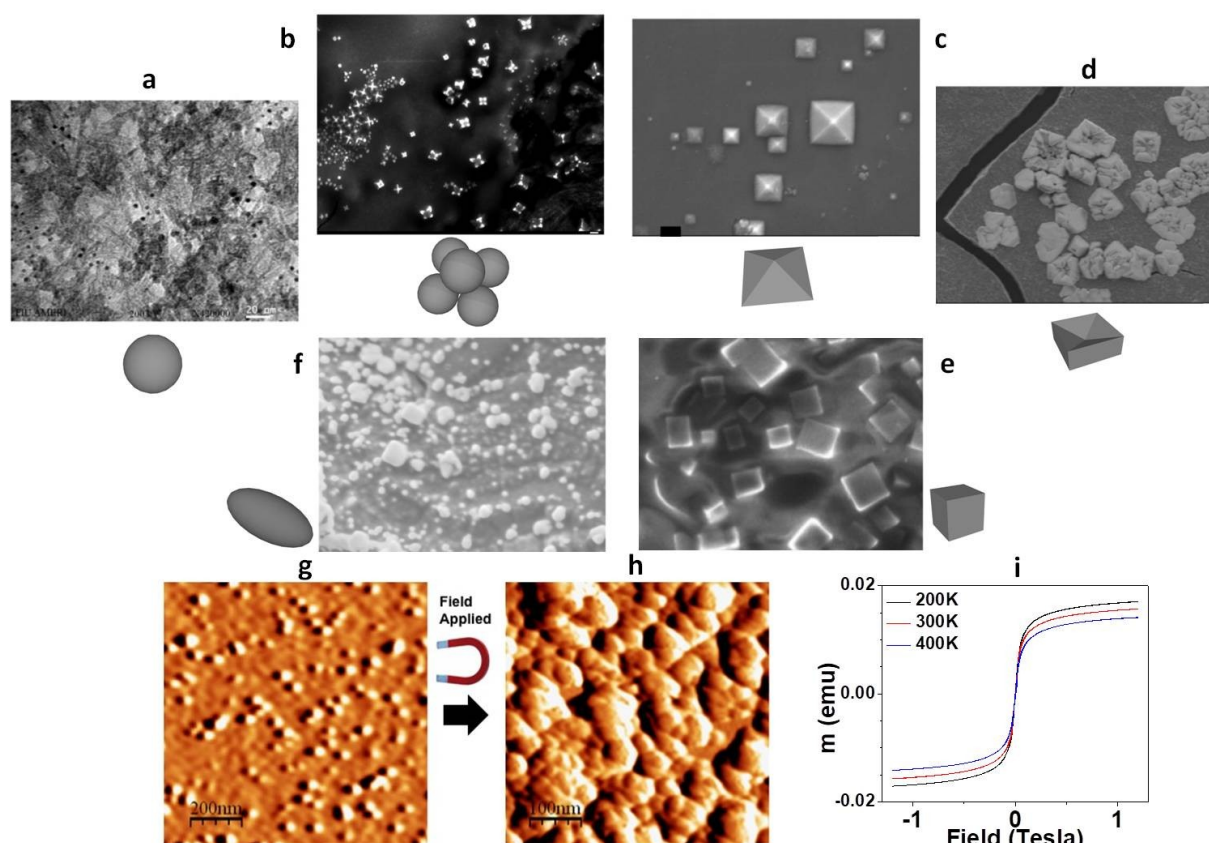


Figure 1 | **Formation and magnetic properties of MNPs.** The shape transformation cycle from circular to hybrid structures of MNPs. **a**, circular shapes. **b**, star shapes. **c**, pyramidal shapes. **d**, negative

pyramidal shapes. **e**, square shapes. **f**, mixed states. **Magnetic properties of MNPs.** AFM images of MNPs **g**, before and **h**, after magnetic field applied. **i**, m-H loops of MNPs with different temperature range.

For the self-aligned nanoparticles using inkjet printing, the nanoparticles need to be chemically stable. To avoid the oxidation state, nanocarbon coating was applied by precisely controlling carbon states such as graphene, nanotubes, and others. Fe-C composites are fabricated by applying high energy milling of iron at low temperature. The method is able to prevent oxidation and may promote Fe nanoparticles without any oxide or impurity. We note that cryo-milling at inert atmosphere has the ability to produce free nanoparticles of metals with minimum contamination.^[23] The present experiments were conducted using Fe powders of 99.999% purity in a specially designed mill under pure Ar.^[23] The cutting and milling is capable of operating at the ranges of $\sim 150\text{K}$ with the help of liquid nitrogen (LN_2) cooling.^[24] The average particle size has been reduced substantially due to cryo-milling and from about $20\ \mu\text{m}$ size of the as-received powder to a size of $\sim 10\ \text{nm}$ after $3\ \text{h}$ of milling. Then, carbon coating was performed through chemical vapor deposition (CVD).^[13] Scanning electron microscopy as shown in **Figures 2a-d** presents the morphology of Fe-C structures by the change of the growth temperature from 1000K , 1100K , 1200K , to 1250K , respectively. One of the particles is chosen for thin film EDS analysis with a fine probe which again indicates that oxygen is absent in the nanoparticles. Moreover, the

electron energy loss spectroscopy (EELS) did not show the presence of oxide as shown in Supplementary Information. However, the analysis of EELS spectra from the edges indicates ~ 0.1 % of oxygen solubility in Fe.

Raman analyses present two distinguished peaks such as *D*- and *G*-peaks, respectively. From the growth temperature at 1000K, the majority peak of Raman spectra shows both *D*- and *G*- peaks. As shown in **Figure 2e**, about 60% particles with several hundreds of nanometers present CNT peaks. The presence of mixed states of CNT and graphene at 1100K. Then, the graphene state is well defined at 1200K, but small CNT peak is also observed. At 1250K, an excellent graphene peak was observed and the roughness is good with tiny CNT peaks as shown in **Figure 2e**.

Without applying magnetic field, it is hard to image the particles due to its topographical nature. Full-field soft x-ray microscopy could distinguish the magnetic properties of Fe and Fe-O states. For the particle imaging, the two images taken at ± 2700 Oe are subtracted to obtain magnetic dichroism. The resonance energies for Fe and Fe-O are 708 eV and 710 eV, respectively. **Figure 2f** shows the x-ray magnetic circular dichroism (XMCD) imaging of the Fe. An image at L_3 edge presents typical metallic behaviors without peak splitting or any signs of oxidation, although the system was exposed to air. The monolayer graphene membrane served as a coating to prevent any strong reaction. Overall, the XMCD signals were also clearly observed. Additional information for further detail will be shown in **Supplementary Information**. Because of the nature of MNPs, it is hard to observe using other imaging techniques, but the full field XMCD

imaging enables it to probe the magnetic properties in an element-specific measurement.

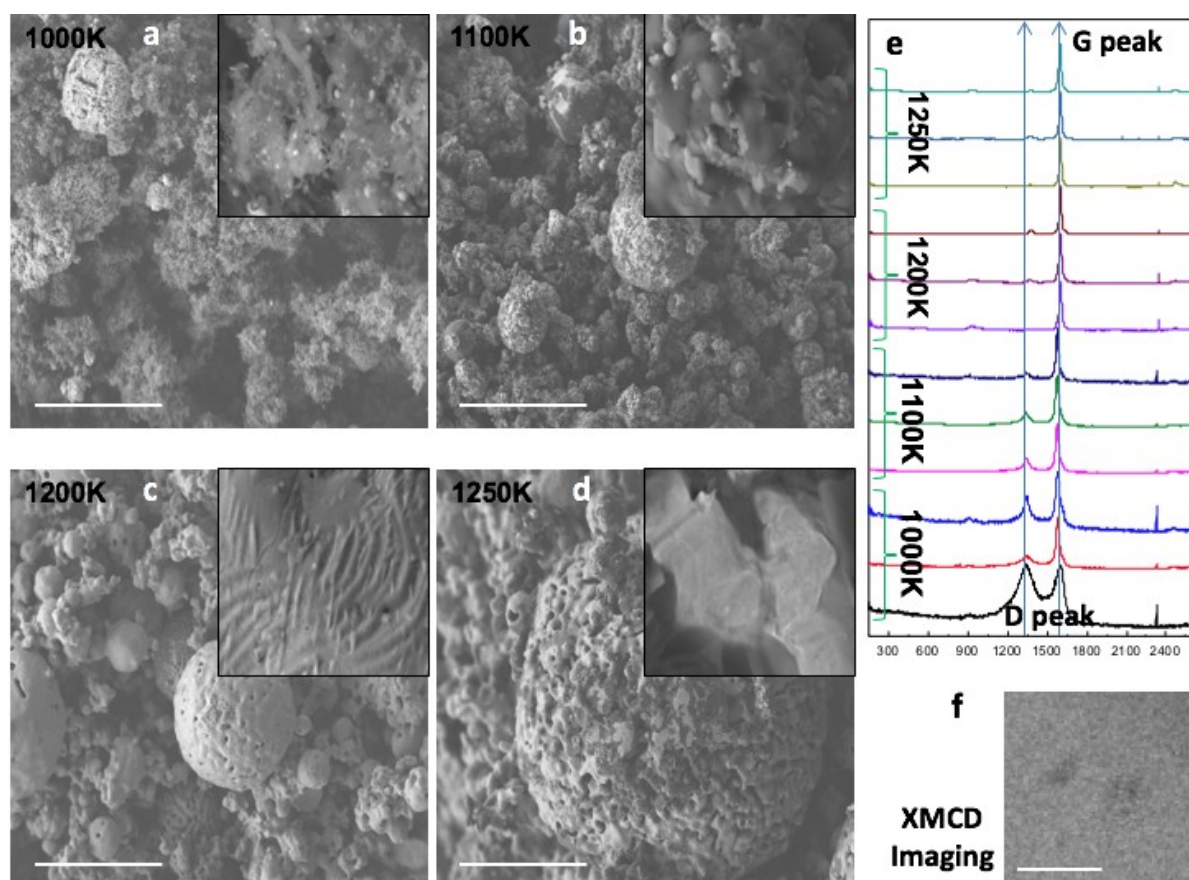


Figure 2 | **Fe-C core-shell structures.** SEM images of Fe-C core-shell structures grown at 1000K (**a**), 1100K (**b**), 1200K (**c**), and 1250K (**d**), respectively. The scale bars are 1 μm . **e**, Raman peaks of different synthesis temperature and time. Notice that the change of **D**- and **G**-peaks by varying the temperature ranges from 1000K to 1250K, respectively. **f**, A full field magnetic micrograph of Fe-C core-shell using synchrotron radiation. Dark regions represent XMCD of Fe-C core-shells. The scale bar is 500 nm .

Although drop casting is a well-known technology to deposit MNPs onto the dry substrates, it is hard to control the distribution of MNPs depending

on the size due to large volume of drops over a few over a few μL . Meanwhile, inkjet printing allows more precise patterning with less volume of droplets ($\sim\text{pL}$) from a nozzle with diameter of tens-of-micrometer. This strategy contains several advantages such as low-cost, easy access to realize electronic devices, and being a precise material dispersion technique with non-contact deposition on a variety of substrates.^[19] After finding the optimal conditions, the prepared MNPs was inkjet-printed onto rigid (silicon) and flexible (Polydimethylsiloxane, *PDMS*) substrates.

The experimental details are described in the **Materials section**. **Figure 3a** shows a schematic and optically captured image of Fe-C MNPs jetting. By optimizing the ejection conditions including voltage pulse amplitude and duration, the droplets in-flight from single nozzle were spherically well defined. **Figure 3b** presents the particles are aligned by size due to the coffee ring effect after dropped onto the substrates. The results with the deposition of Fe-C particles present the structures are well aligned. The size controllable effects will be discussed more in detail in **Supplementary Information**. Using inkjet printing, we can control the size and distribution of MNPs as shown in **Figure 3c**. **Figure 3d** shows that the MNPs are well aligned in a uniform way. The size distribution presents the uniform arrays of nanoparticles having a diameter of sub-10-nm are aligned in the middle region. When it is deposited on a PDMS substrate, it was observed that the MNPs are well aligned. Left and right images of **Figure 3d** shows SEM and AFM images of MNPs deposited on PDMS substrate, respectively.

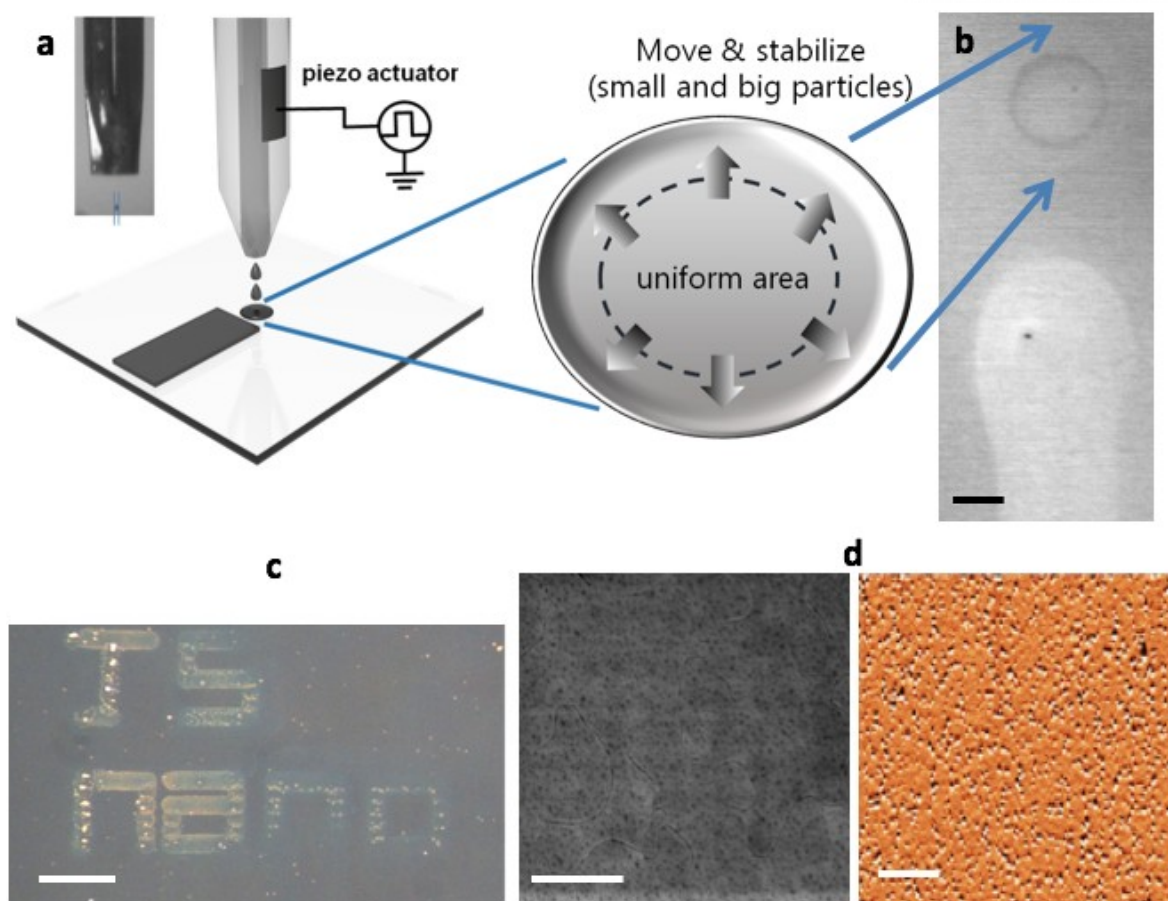


Figure 3 | **Distribution of the MNPs through inkjet printing.** **a**, A schematic of inkjet jetting image which shows micro-sized Fe-C solution drops. The volume of ejected single droplet is $60 \mu\text{L}$ from the nozzle having a diameter of $30 \mu\text{m}$. **b**, An optical microscopy image of MNP single drop (top) and line (bottom) formation onto Si substrate. When exploiting the coffee ring effects, the particles are aligned by uniform size. **c**, Using optimal drops and lines, the drop-on demand printing was performed. Scale bar is 2 mm . **d**, The resulting images of uniformly arrayed Fe-C structures onto PDMS taken by SEM (L) and AFM (R). The scale bar is $2 \mu\text{m}$.

We found three important milestones for MNPs. First, the formation of self-assembled 3D pyramidal nanoparticles could be optimized by changing the process conditions. We could control the formation of four phases of

the self-assembled 3D nanodevices such as pyramidal, square, hybrid, and circular nanostructures. Second, Fe-C particles could prevent oxidation and show strong XMCD images at Fe L_3 edge. That means carbon prevent the penetration of any atoms into Fe core. Last, we applied inkjet printing to align MNPs. The MNPs were aligned in a size controllable and uniform way onto flexible substrates. The results pave the way to the field of nanoparticles based future electronics and smart medicine.

Experimental Section

Nanomagnetic Particle Fabrication: Nanomagnetic particles were fabricated through coprecipitation from a solution of ferrous and ferric mixed salts in the ratio of 1:2 under ambient conditions of the bulk aqueous solution and surfactant systems.^[4,16] De-ionized water (300 mL) was deaerated in a three-necked flask through stirring with the application of ultra-high-purity nitrogen. First, 2 g of hydrated ferrous chloride, $\text{FeCl}_2 \cdot 2\text{H}_2\text{O}$, was mixed with 5.4 g of hydrated ferric chloride, $\text{FeCl}_3 \cdot 6\text{H}_2\text{O}$, in 300 mL of water, and was dissolved at 30–40 °C. Then, a solution of 5 g NaOH in water at 50 °C was added at a constant stirring rate of 2000 rpm, and a black magnetite precipitate was deposited.

Transmission Electron Microscopy: A transmission electron microscope (TEM; Philips CM-200) with an acceleration voltage of 200 kV was used to take TEM images. A field-emission gun equipped with a Gatan GIF200 imaging filter running DigitalMicrograph™ software was used. TEM samples were prepared by placing a drop of mini-emulsion onto a carbon-coated copper grid under ambient conditions.

X-ray Diffraction: X-ray diffraction (XRD) measurements were taken using a Siemens D-5000 diffractometer equipped with a Cu anode operated at 40 kV and 40 mA. The XRD patterns were collected with a step size of 0.01° and a scan rate of 1 step/s. Data were analyzed from the Powder Diffraction File (PDF).

Scanning Electron Microscopy: Scanning electron microscopy was performed with a JEOL 9000F instrument at 15 kV and a working distance of 5 mm.

Vibrating Sample Magnetometry: m-H loop measurements were performed using the VSM option of a Quantum Design cryogenic physical property measurement system (PPMS) with a 9 T superconducting magnet. Samples were mounted in a regular tube holder. To optimize the touchdown process, the samples were mounted with an upward offset of 35 mm. The magnetic field was swept at the rate of 15 Oe/sec.

Magnetic Force Microscopy: The atomic force microscopy (AFM) study was performed in non-contact mode with a Veeco Multimode system. High sensitivity magnetic tunnel junction probes (2 nT/Hz) at 50 Hz was provided from JS Nanotechnologies (San Jose, CA). The particle imaging was performed in standard SPM system.

XM-1 Microscopy: XMCD was imaged using full-field soft x-ray transmission microscopy at Lawrence Berkeley National Lab, Advanced Light Source, Beamline 6.1.2 along the Fe (708 eV) absorption edge. In order to clearly identify current-induced motion of magnetic textures, an area of the wire with an artifact within the field of view was chosen to

facilitate alignment between image snapshots. Each snapshot is the result of a 2 sec exposure and 5 averages.

Inkjet Printing: MNPs were printed on a 60 °C substrate using a customized drop-on-demand piezoelectric-type inkjet printing system with MJ-AT-01 nozzles from MicroFab Corp. The experimental conditions are based on the following parameters: concentrations, types of solvent, substrate temperature, and drop spacing. We tried different conditions which are 0.1, 0.5, and 1.0 *g/mL* concentrations, respectively by changing different solvent of IPA and Acetone. The temperature range of the substrates was 50, 60, and 70 °C, respectively. The variations of drop spacing were performed from 30 to 180 μm . Using the optimal results, we deposited MNPs onto different substrates such as rigid and flexible substrates.

The addition of new functions of Fe-based nanoparticles such as shape transformation, oxidation prevention, and self-alignment could be controllable for their shape by oxidation states and properties through nanocarbon coating.

Keywords: Core-shell; Fe nanoparticles; Fe-C nanostructures; Magnetic nanoparticles; inkjet printing